The Pharmaceutical and Chemical Journal, 2020, 7(3):90-99

Available online www.tpcj.org

Research Article

ISSN: 2349-7092
CODEN(USA): PCJHBA

A Density Functional Theory Study on Molecular Structure and Infrared Spectrum for Antimycobacterial [Pd(C-bzn)(SCN)(dppp)] Compound

Osvaldo Treu-Filho[1], Luã F S de Oliveira[1], Helieverton G de Brito[1], Hérica C Cordeiro[1], José Ciríaco-Pinheiro[1]*, Fábio dos S Gil[1], Márcio de S Farias[1], Raimundo D P Ferreira[1], Marcos A B dos Santos[2], Antonio F de Figuiredo[3]

[1]Laboratório de Química Teórica e Computacional, Faculdade de Química, Instituto de Ciências Exatas e Naturais, UFPA, CP 10101, CEP 66075-110 Belém, PA, Brasil
[2]Departamento de Ciências Naturais, Universidade do Estado do Pará, UEPA, CEP 68477-000 Barcarena, PA, Brasil
[3]Instituto Federal de Educação Tecnológica do Pará, IFPA, CEP 68740-970 Castanhal, PA, Brasil
*Corresponding author:E-Mail:ciriaco@ufpa.br (J. C. Pinheiro).

Abstract The organometallic compound [Pd (C-bzan) (SCN) (dppp)] {bzan=N-benzylideneaniline, dppp = 1,3-bis(diphenylphosphino)propane} with antimycobacterial activity was studied by the Handy's OPTX modification of Becke's exchange functional by using the Vosko, Wilk, and Nusair 1980 correlation functional (III) quantum chemical approach. The theoretical geometric parameters showed that the coordination geometry of the palladium atom is square planar, through two phosphorus atoms of the dppp ligand, one terminal thiocyanate ligand and one bzan molecule coordinated as a monodentate ligand by the C_7 atom. The molecular electrostatic potential map, the highest occupied molecular orbital and the lowest unoccupied molecular orbital were used in an attempt to identify key structural features of the molecule that are necessary for its biological activity and to investigate the interaction with the molecular receptor. For the infrared spectrum, the comparison between the calculated values and literature data shows a good agreement between the theoretical results and the experimental data.

Keywords [Pd(C-bzn)(SCN)(dppp)] compound; *Mycobacterium tuberculosis;* Density functional theory study; Molecular electrostatic potential map; Infrared spectrum

1. Introduction

Tuberculosis (TB) remains a major global health problem and, every year, millions of people are infected worldwide, turning TB the second leading cause of death by infectious diseases, only surpassed by the Acquired Immunodeficiency Syndrome (AIDS). The infection is caused by *Mycobacterium tuberculosis* and about a third of the world population, according to literature, already has latent TB and it is estimated that ten percent will develop the disease in their lifetime, and, therefore, it is difficult to eradicate it in short term [1-2]. The antitubercular chemotherapy comprises an initial intensive two-month regime with rifampicin, isoniazid, pyrazinamide, and ethambutol, or streptomycin, aiming at avoiding the appearance of mutants resistant to a single drug [3-4]. The appearance of multidrug-resistant strains of *M. tuberculosis* (MDRTB) and the need of drugs that also have effectiveness against human immunodeficiency virus infection put on the agenda the urgency in searching for new drugs to treat the disease concomitantly with drugs of antiviral chemotherapy [1,5,6]. Literature has reported that the

introduction of metal ions for the development of new medicinal agents with novel mechanisms of action offers a potentially attractive and ample research area [7-9].

In previous work, we have uses the Becke three-parameter hybrid method [10] using the Lee-Yang – Parr correlation functional [11] (B3LYP) to investigate theoretically the molecular structure and the vibrational spectrum of [Pd (dmba) (NCO) (imz)] [12], cis-[$PdCl_2$ (tmen)], and cis-[Pt $(N_3)_2$ (tmen)] [13] compounds. In this article, we present the computational study of [Pd (C-bzan) (SCN) (dppp)] {bzan=N-benzylideneaniline, dppp = 1,3-bis(diphenylphosphino)propane} compound with antimycobacterial activity against TB bacillus [9]. In our study, the geometry of the compound is computed and compared to experimental data from literature [9]. The molecular electrostatic potential (MEP) [14–19] map is constructed and evaluated in the region where the chelating coordination mode of the dppp ligand occurs, what may be responsible for the biological activity of the antimicrobial activity [9]. Nonetheless, the unawareness of biological target precludes the interaction calculation between the ligand molecule and the biological receptor so as to clarify how the ligand/receptor complex is formed. For that reason, we can suppose that there is a chance the attack of the target occurs in the ligand region with the lowest/or highest electrostatic potential. Then, the highest occupied molecular orbital (HOMO) and the lowest unoccupied molecular orbital (LUMO) [20] are also described and the hypothesis of reactions by electrons transfer of the respective HOMO of the ligand to the LUMO of the biological target or of the HOMO of biological target to LUMO of the ligand are evaluated. Finally, the theoretical harmonic frequencies, infrared (IR) intensities, and normal modes of vibration are shown and compared with some available values in literature [9].

2. Computational

2.1. Theoretical approach and atomic basis

In our investigation, the Handy's OPTX modification of Becke's exchange functional [21,22] by using the Vosko, Wilk, and Nusair 1980 correlation functional (III) [23] quantum chemical approach was employed to determine the properties of interest. For H (^{2}S), C (^{3}P), N (^{4}S), S (^{3}P), and Pd(^{1}S) atoms, we used the wave functions from literature [12, 24]. For P (^{4}S) atom [25], the basis set was designed following the strategy previously reported [24]. The molecular calculations were carried out on C_1 symmetry, electronic state ^{1}A, by using the GAUSSIAN 09 routine [26], and the geometry optimization was computed by using Berny [27].

2.2. The molecular electrostatic potential as a tool to study biological recognition processes

According to literature, two important classes of biological processes, in which the initial step is "recognition", are the drug-receptor and enzyme-substrate interactions; the receptor of the enzyme "recognizes" that an approaching molecule has certain key features that will promote reciprocal interaction. Such recognition is believed to take place typically when the drug and receptor, or enzyme and substrate, are at a relatively large separation [19].

We can look at the electrostatic potential of a molecule as a significant physical representation of how it is found by a system in its neighborhood, in the search for characteristics that determine whether a particular recognition will occur or not. The MEP has effectively shown to be a tool for the analysis and elucidation of recognition processes. The MEP is related to the electronic density and it is a very useful descriptor to understand sites for electrophilic attack and nucleophilic reactions as well as for hydrogen bonding interactions. Being a real physical property, $V(\vec{r})$ can be determined experimentally by diffraction or by computational methods. A deeper and detailed description of these matters can be elsewhere [15-19].

To investigate the reactive sites of antimycobacterial [Pd(C-bzn)(SCN)(dppp)] compound , the MEP was evaluated using the B3LYPmethod [21-22]. The MEP, at a given point (*x*,*y*,*z*) in the vicinity of a molecule, is defined in terms of the interaction energy between the electrical charge generated from the molecule by electrons and nuclei and a positive test charge (a proton) located at $\vec{r}$. For the studied compound, the $V(\vec{r})$ values were calculated as described previously by using Eq. (1)

$$V(\vec{r}) = \sum_{i=1}^{N} \frac{Z_i}{|\vec{R}_i - \vec{r}|} - \int \frac{\rho(\vec{r}')d\vec{r}'}{|\vec{r}' - \vec{r}|} \qquad (1)$$

where N is the number of nuclei with charges Z_i , located at position R_i and ρ ($\vec{r}$) is the electronic charge density. The first term in (1) represents the contribution of the nuclei, which is positive, and the second term includes the electronic density, which is negative.

The MEP map, computed from the electronic density, the HOMO and the LUMO are displayed with MOLEKEL software [28].

2.3. Frontier molecular orbitals

It has been shown that HOMO and LUMO play a major role in governing many chemical reactions and determine electronic bands gaps in solids. They are also responsible for the formation of many charge-transfer complexes [20]. According to the frontier molecular orbital theory of chemical reactivity, the formation of transition state occurs due to an interaction between the frontier orbitals (HOMO and LUMO) of reacting species [20]. Thus, the treatment of the frontier molecular orbitals separately from other orbitals is based on the general principles that govern the nature of chemical reactions [20]. The energy of HOMO is directly related to the ionization potential and characterizes the susceptibility on the molecule toward attack by electrophiles. The energy of LUMO is directly related to the electron affinity and characterizes the susceptibility of the molecule toward attack by nucleophiles. Both the HOMO and the LUMO energies are important in radical reactions. The concept of hard and soft nucleophiles and electrophiles has been also directly connected to the related energy of HOMO and LUMO. Hard nucleophiles have a low-energy HOMO; soft nucleophiles have a high-energy HOMO; hard electrophiles have a high-energy LUMO; and soft electrophiles have a low-energy LUMO [20].

2.4. Infrared spectrum

The infrared spectrum was calculated by using a harmonic field,[29] and frequency values are not scaled. The principal infrared–active fundamental mode assignments and descriptions were performed by GaussView graphics routine [30].

3. Results and Discussion

3.1. Structure of compound

In Fig. 1, the structure calculations for [Pd(C-bzn)(SCN)(dppp)] compound are shown. The comparison between experimental and the theoretical geometric parameters (Table 1) shows that the coordination geometry about the palladium atom is square planar, through two phosphorus atoms of the dppp ligand, one terminal thiocyanate ligand and one bzan molecule coordinated as a monodentade ligand by the C_7 atom, which reproduce the experimental data reported in literature [9].

Figure 1: Computed structure for [Pd(C-bzn)(SCN)(dppp)] compound

The calculated bond angles around the Pd atom are close to the experimental data. Inside the chelate ring, the experimental and theoretical distances differ, probably as a result of the presence of the bzan ligand. For the terminal thiocyanate, the theoretical and experimental distances are closer as well as the linear S-C-N angle. The theoretical value of the Pd-N (bzan ligand) distance is 2.937 Å, with reasonable agreement to the experimental data (2.729 Å), also indicating a weak interaction between them.

Table 1: Theoretical and experimental geometric parameters of [Pd(C-bzan)(SCN)(dppp)] compound

Geometric parameters	Experimental [9]	Theoretical
Bond lengths (Å)		
Pd_5-P_4	2.355	2.544
Pd_5-P_2	2.255	2.416
Pd_5-S_6	2.423	2.511
N_{76}-C_{75}	1.130	1.182
S_6-C_{75}	1.645	1.674
Bond angles (degree)		
P_2-Pd_5-C_7	85.80	86.67
P_2-Pd_5-P_4	94.45	93.74
S_6-Pd_5-C_7	87.30	86.15
S_6-Pd_5-P_4	92.71	91.72
S_6-C_{75}-N_{76}	77.30	177.80

3.2 MEP map for compound

The analysis of the MEP map (Fig 2) shows a surface map around of the N atom(NCS), characterized by negative electrostatic potential (red color), whose the lowest values for charge were -0.221au (atomic unit); this must be the ligand region susceptible to the biological receptor nucleophilic attack. Other regions of the molecule have contour surface (green color), characterized by positive electrostatic potential with small values, and, for the contour surface (blue color), the highest values for charge were +0.259 au. The electron density around the N atom (NCS) can induce the molecule to show antimicrobial activity, suggesting a complexation of the N atom (NCS) with the active site of the biological receptor. However, as the biological target is unknown, it is not possible to study the ligand/receptor interaction using the molecular docking, and, therefore, we can suppose, hypothetically, that the biological process occurs when the receptor attacks the highest electrostatic potential region of the ligand (+0.259 au).

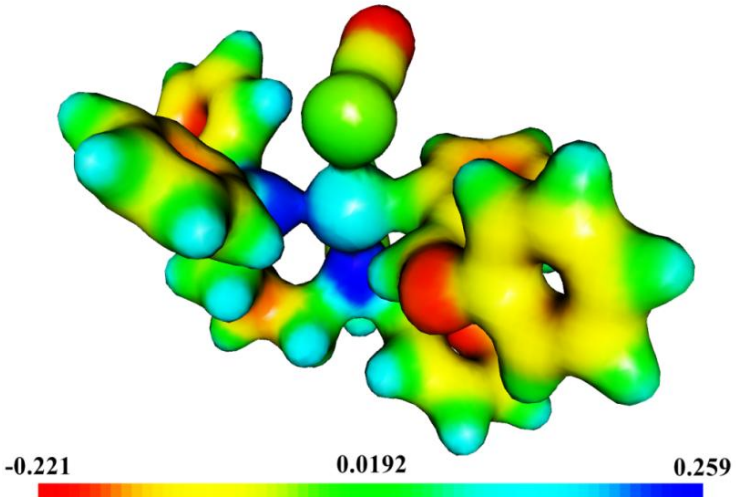

Figure 2: MEP map (in atomic unit) for the [Pd(C-bzn)(SCN)(dppp)] compound

3.3. HOMO and LUMO orbitals for the compound

Fig. 3 shows the HOMO (a) and the LUMO (b) orbitals for the [Pd(C-bzn)(SCN)(dppp)] compound.

In this figure, we can see that the HOMO orbital (Fig. 3a) is located essentially in regions of the molecule containing Pd atom and cyanate group and presents the contribution in the P_2[-0.12 $3p_x$], Pd_5[-0.12 $4d_{xx}$], S_6[+0.53 $3p_x$ + 0.16 $3p_y$], C_{17}[+0.16 2s], N_{19}[+0.15 2s - 0.10 $2p_x$ - 0.11 $2p_z$], C_{20}[+0.38 2s], C21[-0.31 2s], C_{22}[+0.24 2s], C_{23}[-0.23 2s], C_{24}[+0.25 2s], C_{25}[-0.35 2s], C_{42}[-0.12 2s], C_{43}[+0.13 2s], C_{45}[+0.10 2s], N_{76}[-0.24 $2p_x$] bonds. The LUMO orbital (Fig.3b) reveals contribution in several regions of the molecule, with principal contributions in the overlaps: P_2[+0.54 3s – 0.35 $3p_x$], C_3[+0.10 2s], P_4[-0.30 3s], Pd_5[-0.25 $4p_y$ + 0.54 $4d_{yx}$ +0.24 $4d_{xz}$ + 0.50 $4d_{x^2-y^2}$ + 0.36 $4d_{xy}$], S_6[+0.29 $3p_y$ - 0.13 $3p_z$], C_7[-0.44 2s + 0.54 $2p_x$ + 0.10 $2p_y$ + 0.13 $2p_z$], C_8[+0.11 2s – 0.12 $2p_z$], C_{11}[-0.13 2s], C_{17}[-0.10 2s], C_{31}[-0.18 2s – 0.11 $2p_x$ + 0.12 $2p_y$], C_{32}[-0.11 2s], C_{33}[+0.22 2s], C_{42}[-0.15 2s], C_{53}[+0.14 2s], C_{64}[+0.31 2s], C_{65}[-0.25 2s], C_{66}[+0.16 2s], C_{67}[-0.14 2s], C_{68}[+0.14 2s], C_{69}[-0.21 2s], C_{75}[-0.11 2s]. For the analysis of HOMO and LUMO, it can be inferred that the molecule has a different interaction, in case of electron donating or receiving, with the active site of the biological receptor.

For the hypothesis of ligand/receptor complex formation due to nucleophilic attack of the biological target in the ligand, we can verify a reaction with electrons transfer from the HOMO of the ligand molecule to the LUMO of the biological target. Oppositely, in order to an electrophilic attack to the ligand molecule occurs, by the biological target molecule, a reaction will be developed with electrons transfer from the HOMO of the receptor to the LUMO of the ligand molecule.

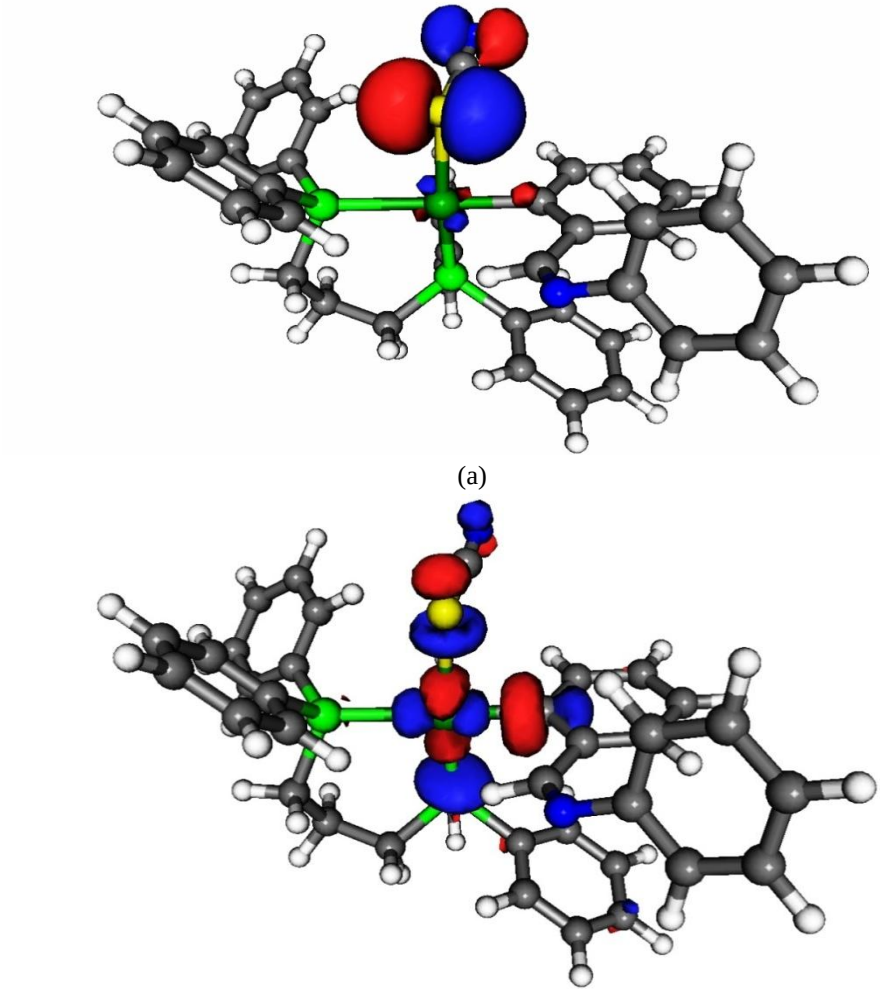

(a)

(b)

Figure 3: HOMO (a) and LUMO (b) orbitals for the [Pd(C-bzn)(SCN)(dppp)] compound

3.4. The infrared spectrum for the compound

Table 2 shows the theoretical IR bands and the most significant intensity. The experimental data reported in literature [9] shows the characteristic bands for S-thiocyanate at 2096 cm^{-1} (υ_{as}NCS) and 827 cm^{-1} (υ_{as}NCS). The dppp ligand shows characteristic bands at 2889 cm^{-1} (νCH2), 1106 cm^{-1} (νPC) and 688 cm^{-1} (γCH), and coordinated N-benzylideneaniline shows absorptions at 1577 cm^{-1} (νC=N) and 744 cm^{-1} (γCH) [9].

The comparison between the calculated values, Table 2, and literature data shows a good agreement between theoretical results and experimental data. The main factor responsible for the discrepancies between the experimental and the computed values is related to the fact that theoretical calculations do not include anharmonics effects in the vibrations of infrared [31-32]. While anharmonicity is the main factor of the discrepancies in the case of vibrations related to the (υ_sNCS) or dppp (υ (CH_2)) bonds, for other vibrations, many of the discrepancies come from the approximated nature of the computational technique used, and probably, also, from the lattice effects in the substance studied as a solid while the theoretical calculations belong to gaseous phase [31,33].

Table 2: Theoretical harmonic frequencies, IR-intensities, and normal modes of vibration of organometallic [Pd(C-bzan)(SCN)(dppp)] compound of C_1symmetry

Frequencies (cm^{-1})	Relative Intensity	Description of the normal modes of vibration
3223	0.01	ν_s (C-H) ring dppp
3211	0.02	ν_s(C-H) ring bzan
3198	0.01	ν_s (C-H) ring dppp
3196	0.03	ν_s (C-H) ring dppp
3189	0.03	ν_s (C-H) ring dppp
3184	0.05	ν_s (C-H) ring dppp
3180	0.05	ν_s (C-H) ring dppp
3179	0.03	ν_s(C-H) ring bzan
3176	0.07	ν_{as} (C-H) ring dppp
3175	0.03	ν_{as} (C-H) ring dppp
3174	0.09	ν_{as} (C-H) ring dppp
3173	0.08	ν_{as} (C-H) ring dppp
3172	0.09	ν_{as}(C-H) ring bzan
3169	0.08	ν_{as} (C-H) ring dppp
3164	0.09	ν_{as}(C-H) ring bzan
3161	0.06	ν_{as}(C-H) ring bzan
3160	0.05	ν_{as} (C-H) ring dppp
3159	0.03	ν_{as} (C-H) ring dppp
3158	0.02	ν_{as} (C-H) ring dppp
3144	0.02	ν_{as} (CH_2) ring bzan
3107	0.04	ν_{as} (CH_2) propane
3097	0.02	ν_{as} (CH_2)propane
3081	0.03	ν_{as} (CH_2)propane
3054	0.04	ν_s (CH_2) propane
3050	0.04	ν_s (CH_2) propane
3041	0.18	ν(C-H) bzan
3013	0.07	ν_s (CH_2) propane
2097	0.23	ν_{as} NCS
1656	1.00	ν(C=N) bzan
1606	0.34	ν_s (C-C) ring bzan
1583	0.12	ν_s (C-C) ring bzan
1564	0.09	ν_{as} (C-C) ring bzan
1496	0.03	δ(C-H)$_{\text{in plane}}$ringdppp
1494	0.11	δ(C-H)$_{\text{in plane}}$ringbzan
1477	0.05	δ(CH_2)$_{\text{scissoring}}$propane

1454	0.05	δ(C-H) $_{\text{in plane}}$ringbzan
1451	0.03	δ(C-H) $_{\text{in plane}}$ringdppp
1447	0.06	δ(C-H) $_{\text{in plane}}$ringdppp
1446	0.03	δ(C-H) $_{\text{in plane}}$ringdppp
1414	0.12	δ(C-H)$_{\text{in plane}}$ringbzan
1331	0.02	$\delta(CH_2)_{\text{wag}}$propane
1288	0.02	$\delta(CH_2)_{\text{wag}}$propane
1277	0.05	δ(C-H)$_{\text{in plane}}$ringbzan
1207	0.04	δ(C-H)$_{\text{in plane}}$ringbzan + δ(C-H) $_{\text{in plane}}$ ringdppp
1191	0.05	$\delta(CH_2)_{\text{wag}}$propane + $\delta(CH_2)_{\text{twist}}$propane
1169	0.10	δ(C-H) $_{\text{in plane}}$ring bzan + ν (C-N) bzan
1109	0.06	δ(C-H) $_{\text{in plane}}$ring bzan
1090	0.02	δ(C-H) $_{\text{in plane}}$ring bzan
1085	0.03	ν (P-C $_{\text{ring}}$) + δ(C-H) $_{\text{in plane}}$ dppp
1082	0.05	ν (P-C $_{\text{ring}}$) + δ(C-H) $_{\text{in plane}}$ dppp
1081	0.06	ν (P-C $_{\text{ring}}$) + δ(C-H) $_{\text{in plane}}$ dppp
1053	0.01	ϕ(ring breathing) dppp
1033	0.02	ϕ(ring breathing) dppp
995	0.21	ϕ(ring breathing) dppp
982	0.14	$\delta(CH_2)_{\text{rocking}}$propane
829	0.10	$\delta(CH_2)_{\text{rocking}}$propane
795	0.08	$\delta(CH_2)_{\text{rocking}}$propane
769	0.04	ϕ(ring breathing) bzan
756	0.08	δ(C-H) $_{\text{out of plane}}$ring bzan
751	0.11	δ(C-H) $_{\text{out ofplane}}$ ring bzan
741	0.04	δ(C-H) $_{\text{out ofplane}}$ ring dppp
739	0.11	δ(C-H) $_{\text{out ofplane}}$ ring dppp
737	0.06	δ(C-H) $_{\text{out ofplane}}$ ring dppp
733	0.12	δ(C-H) $_{\text{out ofplane}}$ ring dppp
708	0.01	ν_s NCS
701	0.06	δ(C-H) $_{\text{out ofplane}}$ ring bzan
691	0.02	ν(P-C $_{\text{ring}}$)
685	0.05	δ(C-H) $_{\text{out ofplane}}$ ring bzan
682	0.04	ν_s(P-C $_{\text{ring}}$)dppp
665	0.06	δ C $_{\text{out ofplane}}$ ring dppp
664	0.04	δ C $_{\text{out ofplane}}$ ring dppp
663	0.05	δ C $_{\text{out ofplane}}$ ring dppp
658	0.03	δ C $_{\text{out ofplane}}$ ring dppp
634	0.02	δ C $_{\text{inplane}}$ ring bzan
622	0.02	δ C $_{\text{inplane}}$ ring dppp
610	0.07	ν_s(P-C) propane
582	0.02	δ N $_{\text{out ofplane}}$ bzan
527	0.03	δ C $_{\text{out ofplane}}$ ring bzan
511	0.03	δ C $_{\text{inplane}}$ ring bzan
508	0.02	ν (P-C) ring dppp
500	0.24	δ(C-H) $_{\text{out ofplane}}$ ring dppp
474	0.05	δ(C-H) $_{\text{out ofplane}}$ ring dppp
461	0.02	δ(C-H) $_{\text{out ofplane}}$ ring dppp
423	0.02	δ(C-H) $_{\text{out ofplane}}$ ring bzan
417	0.06	δ C $_{\text{inplane}}$ thiocyanato group + δ $(CH)_{2\text{rocking}}$
411	0.04	ν (P-Pd)

4. Concluding remarks

We have explored the DFT theory to study the molecular structure and the IR spectrum of the antimycobacterial [Pd (C-bzn) (SCN) (dppp)] compound. The results show that the coordination geometry about the palladium atom is square planar. The electron density around the N atom (NCS) can induce the molecule to show antimicrobial activity, suggesting a complexation of the N atom (NCS) with the active site of the biological receptor, whether an nucleophilic attack of the receptor to the ligand molecule occurs (red color in MEP map -0.221 au). Also, the possibility of a nucleophilic attack of the biological target, with the HOMO electron transfer from the ligand molecule to the LUMO of the biological receptor, or an electrophilic attack of the ligand molecule, with HOMO electron transfer from the biological receptor to the LUMO of this molecule can be verified. In addition, the calculated values for the IR spectra show a good agreement with the experimental data.

Acknowledgments

We acknowledge the financial support of Coordenação de Aperfeiçoamento de Pessoal do Ensino Superior (CAPES) and Conselho Nacional de Desenvolvimento Científico e Tecnológico (CNPq). We also thank the Centro Nacional de Processamento de Alto Desempenho (CENAPAD-UNICAMP), the Laboratório de QuímicaTeórica e Computacional (QTC-UFPA) and the Swiss Center for Scientific Computing for the use of the Molekel software.

This work is dedicated to Rogério Toshiaki Kondo (in memory) of the Centro de Informática de São Carlos of the Universidade de São Paulo (USP) for his contributions to our group in various scientific research.

References

[1]. Global tuberculosis report 2018. Geneva: World Health Organization: 2018. Licence:CCBY-NC-SA3.0IGO. https://apps.who.int/iris/bitstream/handle/10665/274453/9789241565646-eng.pdf. Accessed 24 April 2020

[2]. Zumla, A., Atun, R., Maeurer, M., Mwaba, P., Ma, Z., O´Grady, J., Bates, M., Dheda, K., Hoelscher, M.,& Grange, J.(2011). Scientific dogmas, paradoxes and mysteries of latent Mycobacterium tuberculosis infection. Tropical Medicine & International Health, 16(1):79 – 83.

[3]. Ducan, K. (2003).Progress in TB drug development and what is still needed. Tuberculosis 83(1-3): 201-207.

[4]. Koul, A., Arnoult, E., Lounis, N., Guillemont, J., & Andries, K. (2011). The challenge of new drug discovery for tuberculosis. Nature 469(7331): 483-490.

[5]. Branco, F. S. C., Pinto, A. C., & Boechat, N. (2012). A Química Medicinal de Novas Moléculas em Fase Clínica para oTratamento da Tuberculose. Revista Virtual de Química 4(3): 287-328.

[6]. Gandhi, N. R., Nunn, P., Dheda, K., ScHaaf, H. S., Zignol, M., van Soolingen, D., Jensen, P., & Bayona, J. (2010). Multidrug-resistant and extensively drug-resistant tuberculosis: a threat to global control of tuberculosis. Lancet 375(9728): 1830-1843.

[7]. Ronconi, L., & Sadler, P. J. (2007).Using coordination chemistry to design new medicines. Coordination Chemistry Reviews 251(13-14):1633-1648.

[8]. Souza, R. A., Stevanato, A., Treu-Filho O., Netto, A. V. G., Mauro, A. E., Castellano, E. E., Carlos, I.Z., Pavan, F. R., & Leite, C. Q. F. (2010). Antimycobacterial and antitumor activities of Palladium(II) complexes containing isonicotinamide (isn): X-ray structure of trans-$[Pd(N_3)_2(isn)_2]$. European Journal of Medicinal Chemistry, 45(11): 4863-4868.

[9]. Ferreira, J. G., Stevanato, A. S., Santana, A. M., Mauro, A. E., Netto, A. V. G., Frem, R. C. G., Pavan, F. R., Leite, C. Q. F., & Santos, R. H. A. (2012). Structure and antimycobacterial activity of the novel organometallic [Pd(C-bzan)(SCN)(dppp)] compound. Inorg Chem Comm 23: 63-66.

[10]. Becke, A. D. (1993). Density-functional thermochemistry. III. The role of exact exchange. The Journal of Chemical Physics 98: 5648–5652.

[11]. Lee, C., Yang, W., & Parr, R. G. (1988). Development of the Colic-Salvetti correlation-energy formula into a functional of the electron density. Physical Reviw B 37(2):785–789.

[12]. Treu-Filho, O., Pinheiro, J. C., Costa, E. B., Ferreira, J. E. V., Figueiredo, A. F., Kondo, R. T., Lucca-Neto, V. A., Souza, R. A., Legendre, A. O., & Mauro, A. E. (2007). Experimental and theoretical study of the compound [Pd(dmba)(NCO)(imz)]. Journal of Molecular Structure 829(1-3):195–201.

[13]. Treu-Filho, O., Pinheiro, J. C., Souza, R. A., Kondo, R. T., Ferreira, R. D. P., Figueiredo, A. F., & Mauro, A. E. (2007). Molecular structures and vibrational frequencies for cis-[PdCl2(tmen)] and cis-[Pd(N3)2(tmen)]: A DFT study. Inorganic Chemistry Communications 10(12): 1501–1504.

[14]. Shafieyoon, P., Mehdipour, E., & Mary, Y. S. (2019). Synthesis, characterization and biological investigation of glycine-based sulfonamide derivative and its complex: Vibration assignment, HOMO – LUMO analysis, MEP and molecular docking. Journal of Molecular Structure 1181: 244–252.

[15]. Scrocco, E., & Tomasi, J. (1979). Electronic Molecular Structure, Reactivity and Intermolecular Forces: An Euristic Interpretation by Means of Electrostatic Molecular Potentials. Advances in Quantum Chemistry 11:115-193.

[16]. Politzer, P., Laurence, P. R., Jayasuriya, K., & McKinney, J. (1985). Molecular electrostatic potentials: an effective tool for the elucidation of biochemical phenomena. Environmental Health Perspectives 61: 191-202.

[17]. Scrocco, E., & Tomasi, J. (1973).The electrostatic molecular potential as a tool for the interpretation of molecular properties. In: New Concepts II. Topics in Current Chemistry Fortschritte der Chemischen Forschung, vol 42. Springer, Berlin, Heidelberg in Current Chemistry. Springer, Berlin.

[18]. Politzer, P., & Truhlar, D. G. (1981).Chemical Applications of Atomic and Molecular Electrostatic Potentials, Plenum, New York.

[19]. Politzer, P., & Murry, J. S. (2002). The fundamental nature and role of the electrostatic potential in atoms and molecules. Theoretical Chemistry Accounts108: 134-142.

[20]. Karelson, M., Lobanov, V. S., & Katritzky, A. R. (1996). Quantum-Chemical Descriptors in QSAR/QSPR Studies. Chemical Reviews 96(3): 1027-1043.

[21]. Handy, N. C., & Cohen, A. J. (2001). Left-right correlation energy. Molecular Physics 99(5):403-412.

[22]. Hoe, W.M., Cohen, A., & Handy, N. C. (2001). Assessment of a new local exchange functional OPTX. Chemical Physics Letters 341(3-4): 319-328.

[23]. Vosko, S. H., Wilk, L., & Nusair, M. (1980). Accurate spin-dependent electron liquid correlation energies for local spin density calculations: a critical analysis. Canadian Journal of Physics 58(8):1200-1211.

[24]. Barra, C. V., Rocha, F. V., Gautier, A., Morel, L., Quilles, M. B., Carlos, I. Z., Treu-Filho, O., Frem, R. G., Mauro, A. E., Netto, A. V. G. (2013). Synthesis, cytotoxicactivity and DNA interaction of Pd(II) complexes bearing N′-methyl-3,5-dimethyl-1-thiocarbamoylpyrazole.Polyhedron 65: 214-220.

[25]. The basis set for P (^{4}S) is 22s14p/9s7p (12,2,1,2,1,1,1,1,1/7,1,1,2,1,1,1) with the discretization parameters: $\Omega_{(s)}$ = -0.387, $\Delta\Omega_{(s)}$ = 0.121, $N_{(s)}$ = 22; $\Omega_{(p)}$ = -0.387, $\Delta\Omega_{(p)}$ = 0.121, $N_{(p)}$ = 14. The scaled parameter used for s and d symmetries is A = 6.0. The polarization function is α_d = 0.378326. Full details about the wave are available upon request to the E-mail address: ciriaco@ufpa.br

[26]. Frisch, M. J., Trucks, G. W., Schlegel, H. B., Scuseria, G. E., Robb, M. A., Cheeseman, J. R., Montgomery, J. A., Vreven, T., Kudin, K. N., Burant, J. C., Millam, J. M., Iyengar, S. S., Tomasi, J., Barone, V., Mennucci, B., Cossi, M., Scalmani, G., Peresson, G. A., Nakatsuji, H., Ishida, M., Nakajima, T., Honda, Y., Kitao, O., Nakai, H.,Klene, M., Li, X., Knox, J. E., Hratchian, H. P., Cross, J. B., Bakken, V., Adamo, C., Jaramillo, J., Gomperts, R., Stratmann, R. E., Yazyev, O., Austinm, A. J., Cammi, R., Pomelli, C., Ochterski, J. W., Ayala, P. Y., Morokuma, K., Voth, G. A., Salvador, P., Dannenberg, J. J., Dapprich, S., Daniels, A. D., Strain, M. C., Farkas, O., Malick, D. K., Abuck, A. D., Ragavachari, K., Foresman, J. B., Ortiz, J. V., Cui, Q., Baboul, A. G., Clifford, S., Cioslowski, J., Stefanov, B. B., Liu, G., Liashenko, A., Piskorz, P., Komaromi, I., Martin, R. L., Fox, D. J., Keith, T., Al-Laham, M. A., Peng, C. Y., Nanayakkara, A., Challacombe, M., Gill, P. M. W., Johnson, B., Chen, W., Wong, M. W., Gonzalez, C., &Pople, J. A. (2016). Gaussian 09, Revision A.02, Gaussian, Inc., Wallingford CT.

[27]. Schegel, H. B. (1989)New Theoretical concepts for understanding organic reactions. Academic, The Netherlands.
[28]. Flukiger, P., Luth, H. P., Portmann, S., &Weber, J. (2000-2001). MOLEKEL 4.3. Swiss Center for Scientific Computing, Manno, Switzerland.
[29]. Goodson, D. Z., Sarpal, S. K., Bopp, P., & Wolfsberg, M. Influence on isotope effect calculations of the method of obtaining force constants from vibrational data. The Journal of Physical Chemistry 86(5): 659-663.
[30]. Nielsen, A. B., & Holder, A. J. (2009).GaussView 5.0, Gaussian Inc., Pittsburg, PA.
[31]. Sundaraganesan, N., Ilakiamani, S., & Joshua, B. D. (2007). FT-Raman and FT-IR spectra, ab initio and density functional studies of 2-amino-4,5-difluorobenzoic acid.Spectrochimica Acta A 67(5): 287–297.
[32]. Karabacak, M., Cinar, M., Kurt, M., & Sundaraganesan, N. (2013).Experimental and theoretical FTIR and FT-Raman spectroscopic analysis of 1-pyrenecarboxylic acid.SpectrochimActaA114:509–519.
[33]. Gökce, H., & Bahçeli, S. (2001). Quantum chemical computations of 1,3-phenylenediaceticacid. Spectrochim Acta A 78(2):8 03–808.